Paradoxes of magnetorotational instability and their geometrical resolution

Oleg N. Kirillov* and Frank Stefani†
Helmholtz-Zentrum Dresden Rossendorf Post Office Box 510119, D-01314 Dresden, Germany
(Received 4 April 2011; revised manuscript received 12 August 2011; published 7 September 2011)

Magnetorotational instability (MRI) triggers turbulence and enables outward transport of angular momentum in hydrodynamically stable accretion discs. By using the WKB approximation and methods of singular function theory, we resolve two different paradoxes of MRI that appear in the limits of infinite and vanishing magnetic Prandtl number. For the latter case, we derive a strict limit of the critical Rossby number. This limit of $\mathrm{Ro_c} = -0.802$, which appears for a finite Lundquist number of $S = 0.618$, extends the formerly known inductionless Liu limit of $\mathrm{Ro_c} = -0.828$ valid at $S = 0$.

DOI: 10.1103/PhysRevE.84.036304 PACS number(s): 47.35.Tv, 47.85.L−, 97.10.Gz, 95.30.Qd

I. INTRODUCTION

Magnetorotational instability (MRI) is the main explanation for the fast formation of stars and black holes, by triggering turbulence and angular momentum transport in accretion disks. In its standard version (SMRI), with a vertical field applied, the instability is nonoscillatory [1–4], while a helical applied magnetic field leads to an oscillatory instability (HMRI) [5].

Both in the astrophysical context [6] as well as in laboratory experiments [7], it is vital to know which laws of differential rotation are susceptible to MRI. The hydrodynamic reference point is Rayleigh's criterion [8], which states that a rotating flow with an outwardly increasing angular momentum is stable. This implies, for example, that a Taylor-Couette (TC) flow of an inviscid fluid between the inner and outer coaxial cylinders of radii $R_\mathrm{i} < R_\mathrm{o}$ and of infinite length that rotate with different angular velocities, $\Omega(R_\mathrm{i})$ and $\Omega(R_\mathrm{o})$, is stable if and only if $R_\mathrm{i}^2\Omega(R_\mathrm{i}) < R_\mathrm{o}^2\Omega(R_\mathrm{o})$. In contrast to this, assuming a perfectly conducting fluid and a vertical magnetic field B_z^0 being applied, Velikhov [1] and Chandrasekhar [2] found the more restrictive condition for stability in the form $\Omega(R_\mathrm{i}) < \Omega(R_\mathrm{o})$. Remarkably, the latter criterion does not depend on the magnetic field strength; that is, in the limit $B_z^0 \to 0$ it does not reduce to Rayleigh's criterion valid for $B_z^0 = 0$. This "curious behavior of ostensibly changing the Rayleigh criterion discontinuously" [9] constitutes the *Velikhov-Chandrasekhar paradox* [10], which implies a dependence of the instability threshold on the sequence of taking the two limits of vanishing magnetic field and vanishing electrical resistivity. Its physical origin has been attributed to the fact that in a fluid of zero resistivity the magnetic field lines are permanently attached to the fluid, independent of the strength of the magnetic field [1,2].

Another paradox of MRI emerges in the opposite limit of vanishing electrical conductivity. This *paradox of inductionless HMRI* [11] refers to the fact that in a helical magnetic field a perturbation can grow exponentially, although the instantaneous growth of the energy of any perturbation must be smaller than in the fieldfree case.

Actually, the astrophysical relevance of HMRI is still debated. At first glance, according to the criterion of Liu *et al.* [12], it could work only for rather steep rotation profiles $\Omega(R)$ with Rossby numbers $\mathrm{Ro} := R(2\Omega)^{-1}d\Omega/dR < 2 - 2\sqrt{2} \simeq -0.828$. This would clearly exclude any relevance of HMRI for Keplerian profiles characterized by $\mathrm{Ro} = -0.75$. It has to be noted, though, that the validity of the underlying local WKB approximation and the possible role of electrical boundaries for extending the applicability of HMRI to higher Rossby numbers are controversial [13]. Surprising new arguments arose recently from investigations of the saturation regime of MRI. For the case of small magnetic Prandtl numbers (as they are typical for protoplanetary disks), Umurhan speculated about a saturated rotation profile with regions of reduced shear, sandwiched by regions of strengthened shear [14]. For those latter regions with steeper than Keplerian profiles, HMRI could indeed become relevant.

In this paper, we find the ultimate upper limit of the critical Rossby number for HMRI and resolve the mentioned paradoxes. We establish that these physical effects sharply correspond to the geometric singularities that are inherent on the stability boundaries of leading-order WKB equations.

II. THE VELIKHOV-CHANDRASEKHAR PARADOX

We start with the local WKB equations for the axisymmetric perturbation of a steady-state rotational flow of a viscous and resistive fluid in the presence of an axial magnetic field that were derived and discussed by several authors [3,15,16]. They can be rewritten in the typical form of a nonconservative gyroscopic system [17]:

$$\ddot{u} + [D + \Omega_0(1+\alpha^2)J]\dot{u} + (N+K)u = 0, \qquad (1)$$

where $u = (u_R, u_\phi)^T$ is the fluid velocity in polar coordinates (R,ϕ). Separating the time dependence according to $u = \tilde{u}\exp(\gamma t)$ yields the eigenvalue problem $L(\gamma)\tilde{u} = 0$ for the growth rate of the perturbation γ, where $L(\gamma) = \gamma^2 I + \gamma[D + \Omega_0(1+\alpha^2)J] + N + K$, I is the 2×2 unit matrix, $N = \Omega_0[\omega_\eta(1+\alpha^2) + \mathrm{Ro}(\omega_\eta - \omega_\nu)]J$,

$$K = \begin{pmatrix} \omega_A^2 + \omega_\nu\omega_\eta & k_{12} \\ k_{12} & \omega_A^2 + \omega_\nu\omega_\eta + 4\alpha^2\Omega_0^2\mathrm{Ro} \end{pmatrix} \qquad (2)$$

with $k_{12} = \Omega_0[\omega_\eta(1-\alpha^2) + \mathrm{Ro}(\omega_\eta - \omega_\nu)]$, and

$$J = \begin{pmatrix} 0 & -1 \\ 1 & 0 \end{pmatrix}, \quad D = \begin{pmatrix} \omega_\nu + \omega_\eta & \Omega_0(1-\alpha^2) \\ \Omega_0(1-\alpha^2) & \omega_\nu + \omega_\eta \end{pmatrix}. \qquad (3)$$

*o.kirillov@hzdr.de
†f.stefani@hzdr.de

In the above equations, $\omega_\nu = \nu k^2$ and $\omega_\eta = \eta k^2$ are the viscous and resistive frequencies, $\omega_A = k_z B_z^0 (\mu_0 \rho)^{-1/2}$ is the Alfvén frequency, k_R and k_z are the radial and axial wave numbers of the perturbation, $k^2 = k_z^2 + k_R^2$, $\alpha = k_z/k$, $\Omega_0 = \Omega(R_0)$, and $\mathrm{Ro} = \mathrm{Ro}(R_0)$, where R_0 is the radial coordinate of a fiducial point for the local stability analysis. We use the convention that $\rho = \text{const}$ is the density of the fluid, $\nu = \text{const}$ is the kinematic viscosity, $\eta = (\mu_0 \sigma)^{-1}$ is the magnetic diffusivity, σ is the conductivity of the fluid, and μ_0 is the magnetic permeability of free space. For $\alpha = 1$, $\omega_\nu = 0$, and $\omega_\eta = 0$, Eq. (1) is similar to the Hill equation for two orbiting mass points connected by a spring [18], a paradigmatic model of SMRI [6,9].

Stable perturbations have $\mathrm{Re}\,(\gamma) \leqslant 0$, provided that γ with $\mathrm{Re}\,(\gamma) = 0$ is a semisimple eigenvalue of $L(\gamma)$. The growing solutions of SMRI are nonoscillatory with $\mathrm{Im}\,(\gamma) = 0$ [4,6,9]. Therefore, $\gamma = 0$ implies that $\det(N + K) = 0$ at the threshold of SMRI, which results in the critical Rossby number (above which the flow is stable):

$$\mathrm{Ro_c} = -\frac{\left(\omega_A^2 + \omega_\nu \omega_\eta\right)^2 + 4\Omega_0^2 \omega_\eta^2 \alpha^2}{4\Omega_0^2 \alpha^2 \left(\omega_A^2 + \omega_\eta^2\right)} = -\frac{(\mathrm{Pm}^{-1} + S^2 \mathrm{Pm}^{-2})^2 + 4\mathrm{Re}^2 \mathrm{Pm}^{-2}}{4\mathrm{Re}^2 (S^2 \mathrm{Pm}^{-2} + \mathrm{Pm}^{-2})}, \qquad (4)$$

where $\mathrm{Re} = \alpha \Omega_0 \omega_\nu^{-1}$ is the Reynolds number, $\mathrm{Pm} = \omega_\nu \omega_\eta^{-1}$ is the magnetic Prandtl number, and $S = \omega_A \omega_\eta^{-1}$ is the Lundquist number. Formula (4) coincides with that derived in [16] from the Routh-Hurwitz criterion [19]; see the appendix.

The Velikhov-Chandrasekhar paradox occurs at infinite Pm and means that in the ideal magnetohydrodynamics (MHD) case ($\omega_\eta = 0$, $\omega_\nu = 0$) the limit $\omega_A \to 0$ yields Velikhov's value $\mathrm{Ro_c} = 0$ as the instability threshold rather than Rayleigh's limit $\mathrm{Ro_c} = -1$ of the nonmagnetic case ($\omega_A = 0$, $\omega_\nu = 0$).

With $\omega_A = \varepsilon \cos\varphi$ and $\omega_\eta = \varepsilon \sin\varphi$ in (4), we obtain

$$\mathrm{Ro_c} = -\frac{(\varepsilon \cos^2\varphi + \omega_\nu \sin\varphi)^2 + 4\alpha^2 \Omega_0^2 \sin^2\varphi}{4\alpha^2 \Omega_0^2}, \qquad (5)$$

which for $\varepsilon \to 0$ reduces to

$$\mathrm{Ro_c} = -\left(1 + \frac{1}{4\mathrm{Re}^2}\right) \sin^2\varphi = -\frac{1 + (2\mathrm{Re})^{-2}}{1 + S^2}. \qquad (6)$$

By introducing the new parameter $\mathrm{Ro}' = [1 + 4\mathrm{Re}^2(1 + 2\mathrm{Ro})](1 + 4\mathrm{Re}^2)^{-1}$ we find that in the $(\omega_A, \omega_\eta, \mathrm{Ro}')$ space Eq. (6) defines a so-called *ruled surface* $(\varepsilon, \varphi) \mapsto (\varepsilon \cos\varphi, \varepsilon \sin\varphi, \cos n\varphi)$ with $n = 2$, which is a canonical equation for the Plücker conoid of degree $n = 2$ [20]. The surface according to Eq. (4) tends to the Plücker conoid when $\varepsilon = \sqrt{\omega_A^2 + \omega_\eta^2}$ goes to zero. This surface is shown in the $(\omega_A, \omega_\eta, \mathrm{Ro})$ space in Fig. 1(a) and in projection to the (ω_A, ω_η) plane in Fig. 1(b) for $\mathrm{Re} = 1$. For each α, ω_ν, and Ω_0 it has the same Plücker conoid singularity, that is, an interval of self-intersection along the Ro axis and two Whitney umbrella singular points at its ends. This singular structure implies nonuniqueness for the critical Rossby number when simultaneously $\omega_A = 0$ and $\omega_\eta = 0$. Indeed, for a given S, tending the magnetic field to zero along a ray $\omega_A = \omega_\eta S$ in the (ω_A, ω_η) plane results in a value of the Rossby number specified by Eq. (6); see Fig. 1(c). The limit value of the critical Rossby number oscillates between the ideal MHD value $\mathrm{Ro_c} = 0$ for $S = \infty$ ($\varphi = 0$) and the nonmagnetic value $\mathrm{Ro_c} = -1 - (2\mathrm{Re})^{-2}$ for $S = 0$ ($\varphi = \pi/2$), which explains the Velikhov-Chandrasekhar paradox.

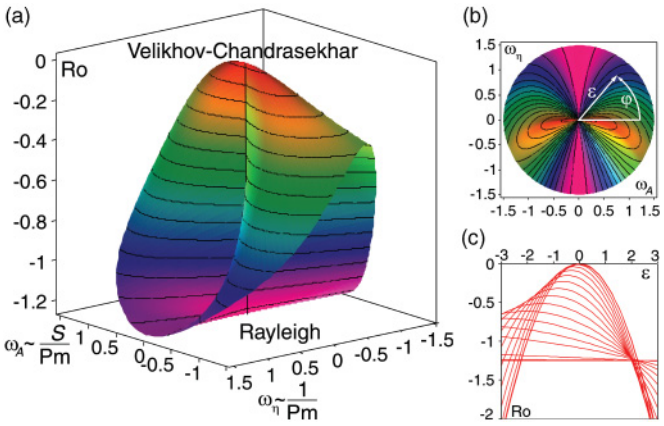

FIG. 1. (Color online) (a) The critical Rossby number of SMRI as a function of $\omega_A \sim S\mathrm{Pm}^{-1}$ and $\omega_\eta \sim \mathrm{Pm}^{-1}$ for $\omega_\nu = 1$, $\alpha = 1$, $\Omega_0 = 1$, i.e., for $\mathrm{Re} = 1$. (b) Top view of the surface. (c) Cross sections of the surface along the rays specified by the Lundquist number, or, equivalently, by the angle φ that varies from 0 to 1.5 through the equal intervals $\Delta\varphi = 0.1$; the horizontal line corresponds to $\varphi = \pi/2$. Note that negative values of ω_η and ε are not physical.

III. THE PARADOX OF INDUCTIONLESS HMRI

Now we turn to the paradox of inductionless HMRI, which is related to a similar geometric singularity as discussed above. The leading-order WKB equations that describe the onset of instability of a hydrodynamically stable TC flow with a helical external magnetic field are $\dot{\xi} = H\xi$ with $\xi^T = [u_R, u_\phi, B_R(\mu_0\rho)^{-1/2}, B_\phi(\mu_0\rho)^{-1/2}]$ and

$$H = \begin{pmatrix} -\omega_\nu & 2\Omega_0\alpha^2 & i\omega_A & -2\omega_{A_\phi}\alpha^2 \\ -2\Omega_0(1+\mathrm{Ro}) & -\omega_\nu & 0 & i\omega_A \\ i\omega_A & 0 & -\omega_\eta & 0 \\ 2\omega_{A_\phi} & i\omega_A & 2\Omega_0\mathrm{Ro} & -\omega_\eta \end{pmatrix}, \qquad (7)$$

where the additional parameter $\omega_{A_\phi} = R_0^{-1} B_\phi^0 (\mu_0\rho)^{-1/2}$ is the Alfvén frequency of the azimuthal magnetic field component [16]. For $\omega_{A_\phi} = 0$ these equations yield (1).

The dispersion equation $\det(H - \gamma I) = 0$ reads

$$\lambda^4 + a_1\lambda^3 + a_2\lambda^2 + (a_3 + ib_3)\lambda + a_4 + ib_4 = 0, \qquad (8)$$

where I is a 4×4 unit matrix, $\lambda = \gamma(\omega_\nu\omega_\eta)^{-1/2}$, and

$$\begin{aligned} a_1 &= 2(1 + \mathrm{Pm}^{-1})\sqrt{\mathrm{Pm}}, \\ a_2 &= 2[1 + (1 + 2\beta^2)\mathrm{Ha}^2] + 4\mathrm{Re}^2(1 + \mathrm{Ro})\mathrm{Pm} + a_1^2/4, \\ a_3 &= a_1[1 + (1 + 2\beta^2)\mathrm{Ha}^2] + 8\mathrm{Re}^2(1 + \mathrm{Ro})\sqrt{\mathrm{Pm}}, \\ a_4 &= \left(1 + \mathrm{Ha}^2\right)^2 + 4\beta^2\mathrm{Ha}^2 + 4\mathrm{Re}^2[1 + \mathrm{Ro}(\mathrm{PmHa}^2 + 1)], \\ b_3 &= -8\beta\mathrm{Ha}^2\mathrm{Re}\sqrt{\mathrm{Pm}}, \quad b_4 = b_3[1 + (1 - \mathrm{Pm})\mathrm{Ro}/2]/\sqrt{\mathrm{Pm}}, \end{aligned} \qquad (9)$$

where we have introduced now the Hartmann number $\mathrm{Ha} = S\mathrm{Pm}^{-1/2}$ and the helicity parameter $\beta = \alpha\omega_{A_\phi}\omega_A^{-1}$ of the

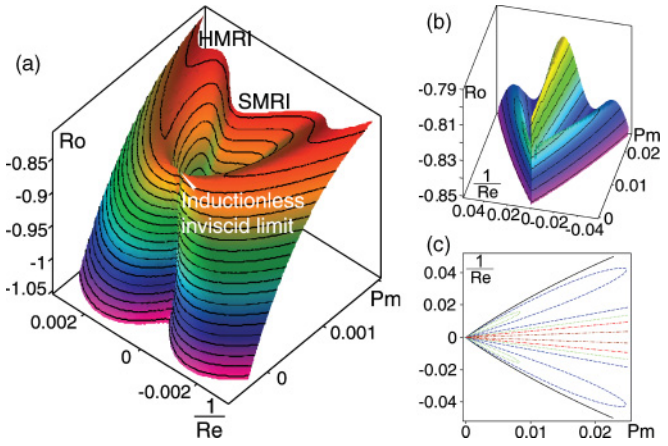

FIG. 2. (Color online) (a) The critical Rossby number of the essential HMRI and helically modified SMRI for $\mathrm{Ha} = 15$ and $\beta = 0.7$ (left) in the $(\mathrm{Pm},\mathrm{Re}^{-1},\mathrm{Ro})$ space. (b) The critical Rossby number for $S = 0.5$ and $\beta = 0.6$ in the $(\mathrm{Pm},\mathrm{Re}^{-1},\mathrm{Ro})$ space and (c) its cross sections in the $(\mathrm{Pm},\mathrm{Re}^{-1})$ plane for (solid black) $\mathrm{Ro} = -0.842$, (dashed blue) $\mathrm{Ro} = -0.832$, (dotted green) $\mathrm{Ro} = -0.822$, (dashed-dotted red) $\mathrm{Ro} = -0.812$, and (dashed-double-dotted brown) $\mathrm{Ro} = -0.802$.

external magnetic field. According to the analog of the Routh-Hurwitz conditions for the complex polynomials—the Bilharz criterion [19]— the threshold of HMRI is defined by $m_4(\beta,\mathrm{Re},\mathrm{Ha},\mathrm{Pm},\mathrm{Ro}) = 0$, where m_4 is the determinant of the so-called Bilharz matrix [16,19] composed of the coefficients (9); see formulas (A2) and (A3) in the appendix. The stability condition $\mathrm{Re}(\lambda) < 0$ holds if and only if $m_4 > 0$ [16,19]. For $\beta = 0$, the dispersion equation and thus the threshold for HMRI reduce to that of SMRI [16].

In the following, we see that in the limit $\mathrm{Pm} \to 0$ it is again S that governs the value of $\mathrm{Ro_c}$. For this purpose, we show in Fig. 2(a) a typical critical surface $m_4 = 0$ in the $(\mathrm{Pm},\mathrm{Re}^{-1},\mathrm{Ro})$ space for the special parameter choice $\mathrm{Ha} = 15$ and $\beta = 0.7$. On the Ro axis, we find a self-intersection and two Whitney umbrella singularities at its ends. At the upper singular point (i.e., exactly at $\mathrm{Pm} = 0$), we get (see [16])

$$\mathrm{Ro_c}(\beta,\mathrm{Ha}) = \frac{(1+\mathrm{Ha}^2)^2 + 4\beta^2\mathrm{Ha}^2(1+\beta^2\mathrm{Ha}^2)}{2\beta^2\mathrm{Ha}^4} - \frac{[(2\beta^2+1)\mathrm{Ha}^2+1]\sqrt{(1+\mathrm{Ha}^2)^2+4\beta^2\mathrm{Ha}^2(1+\beta^2\mathrm{Ha}^2)}}{2\mathrm{Ha}^4\beta^2}. \quad (10)$$

In the limit $\mathrm{Ha} \to \infty$, this critical value is majorated by

$$\mathrm{Ro_c}(\beta) = \frac{1+4\beta^4-(1+2\beta^2)\sqrt{1+4\beta^4}}{2\beta^2}, \quad (11)$$

with the maximum at the well-known Liu limit $\mathrm{Ro_c} = 2 - 2\sqrt{2} \simeq -0.828$ when $\beta = \sqrt{2}/2 \simeq 0.707$ [12,16].

In Fig. 2(a) we see that the case with $\mathrm{Pm} = 0$ is connected to the case $\mathrm{Pm} \neq 0$ by the Plücker conoid singularity, quite similar to the way it was discussed for the paradox of Velikhov and Chandrasekhar. Interestingly, $\mathrm{Ro_c}$ for the onset of HMRI can increase when Pm departs from zero, which happens along curved pockets of HMRI; see Fig. 2(a). The two side bumps of the curve $\mathrm{Re}^{-1}(\mathrm{Pm})$ in a horizontal slice of the surface correspond to the domains of the *essential HMRI* while the central hill marks the *helically modified SMRI* domain, according to the classification introduced in [16]. For small Pm the essential HMRI occurs at higher Ro than the helically modified SMRI, while for some finite value of Pm the central hill and the side bumps get the same value of $\mathrm{Ro_c}$. Most remarkably, there is a value of $\mathrm{Ro_c}$ at which the two side bumps of the curve $\mathrm{Re}^{-1}(\mathrm{Pm})$ disappear completely. This is the maximal possible value for the essential HMRI, at least at the given β and Ha. Now we can ask: How does this limit behave if we send Ha to infinity, and to which value of S does this correspond?

IV. EXTENSION OF THE LIU LIMIT TO THE CASE Pm ≠ 0

Actually, with the increase in Ha the stability boundary preserves its shape and simultaneously it compresses in the direction of zero Pm. Substituting $\mathrm{Ha} = S\mathrm{Pm}^{-1/2}$ into Eqs. (9), we plot again the surface $m_4 = 0$ in the $(\mathrm{Pm},\mathrm{Re}^{-1},\mathrm{Ro})$ space, but now for a given β and S; Fig. 2(b).

The corresponding cross sections of the instability domain in the $(\mathrm{Re}^{-1},\mathrm{Pm})$ plane are shown in Fig. 2(c). At a given value of Ro, there exist three domains of instability with the boundaries shown by the dashed blue and dotted green lines. Two subdomains that have a form of a petal correspond to the HMRI. They are bounded by closed curves with a self-intersection singularity at the origin. They are also elongated in a preferred direction that in the $(\mathrm{Re}^{-1},\mathrm{Pm})$ plane corresponds to a limited range of the magnetic Reynolds number $\mathrm{Rm} = \mathrm{PmRe}$. The central domain, which corresponds to the helically modified SMRI, has a similar singularity at the origin and is unbounded in the positive Pm direction. In comparison with the central domain, the side petals have lower values of Rm.

Now we reconsider again the limit $\mathrm{Pm} \to 0$, while keeping S as a free parameter. At the origin, all the boundaries of the petals can be approximated by the straight lines $\mathrm{Pm} = \mathrm{RmRe}^{-1}$. Substituting this expression into equation $m_4 = 0$, we find that the only term that does not depend on Pm is a polynomial $Q(\mathrm{Rm},S,\beta,\mathrm{Ro}) = p_0 + p_1\mathrm{Rm}^2 + p_2\mathrm{Rm}^4 + p_3\mathrm{Rm}^6$, where the coefficients of the polynomial are given explicitly by formula (A10) in the appendix.

The roots of the polynomial are coefficients Rm of the linear approximation to the instability domains at the origin in the $(\mathrm{Re}^{-1},\mathrm{Pm})$ plane. Simple roots mean nondegenerate self-intersection of the stability boundary at the origin. Double roots correspond to a degeneration of the angle of the self-intersection when it collapses to zero, which happens only at the maximal critical Rossby number, Fig. 2(b). In the (S,β,Ro) space a set of points that correspond to multiple roots of the polynomial Q is given by the discriminant surface $64\Delta^2 p_0 p_3 = 0$. An explicit form for Δ can be found in the appendix; see formulas (A11)–(A14). The surface $p_3 = 0$ consists of a sheet $\mathrm{Ro} = -(1+S^2)^{-1}$ corresponding to the doubly degenerate infinite values of Rm at the maxima of the helically modified SMRI. It smoothly touches along the β axis the surface $\Delta = 0$ that consists of two smooth sheets that touch each other along a spatial curve—the cuspidal edge—corresponding to triple roots of the polynomial Q; see Fig. 3(a).

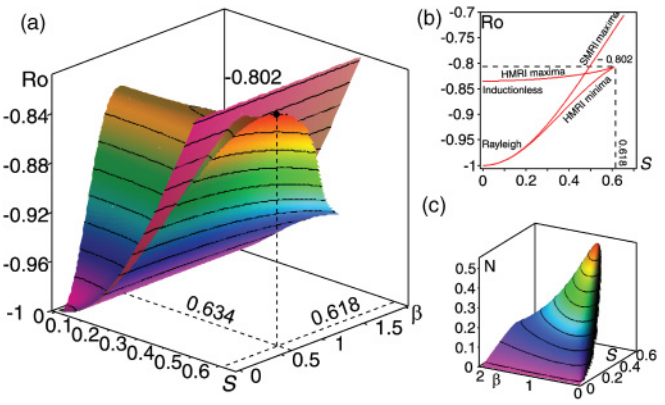

FIG. 3. (Color online) (a) Discriminant surface in the (S,β,Ro) space and (b) its cross section at $\beta = 0.634$. (c) Interaction parameter $\mathrm{N} = S^2\mathrm{Rm}^{-1}$ at the essential HMRI maxima.

Every point on the upper sheet of the surface $\Delta = 0$ represents a degenerate linear approximation to the essential HMRI domain and therefore a maximal Ro at the corresponding values of β and S. Numerical optimization results in the new ultimate limit for HMRI $\mathrm{Ro_c} \simeq -0.802$ at $S \simeq 0.618$, $\beta \simeq 0.634$, and $\mathrm{Rm} \simeq 0.770$; see Fig. 3(b). This new limit of $\mathrm{Ro_c}$ on the cuspidal edge is smoothly connected to the inductionless Liu limit by the upper sheet of the discriminant surface, which converges to the curve (11) when $S = 0$. We point out that the new limit is achieved at $\mathrm{Ha} \to \infty$ when the optimal Pm tends to zero in such a way that $S \simeq 0.618$. Figure 3(c) shows the behavior of the so-called interaction parameter (or Elsasser number) $\mathrm{N} = S^2/\mathrm{Rm}$ for the HMRI sheet. It is remarkable that, at $S = 0$, HMRI starts to work already at $\mathrm{N} = 0$. This can be explained by the observation that the optimal value for HMRI corresponds to $\mathrm{NHa} = S^3/(\mathrm{Rm}\sqrt{\mathrm{Pm}}) = 1/(1 + 2^{-1/2}) = 0.586$ [16]. Later, for increasing S, the optimal N acquires final values, passes through its maximum, and at $S \simeq 0.618$ and $\beta \simeq 0.634$ it terminates at $\mathrm{N} = 0.496$.

V. CONCLUSIONS

Inspired by the theory of dissipation-induced instabilities [17], we have resolved the two paradoxes of SMRI and HMRI in the limits of infinite and zero magnetic Prandtl numbers, respectively, by establishing their sharp correspondence to singularities on the instability thresholds. In either case, it is the local Plücker conoid structure that explains the nonuniqueness of the critical Rossby number and its crucial dependence on the Lundquist number. For HMRI, we have found an extension of the former Liu limit $\mathrm{Ro_c} \simeq -0.828$ (valid for $S = 0$) to a somewhat higher value $\mathrm{Ro} \simeq -0.802$ at $S = 0.618$, which is, however, still below the Kepler value. Studying the possible consequences of this new limit for the saturation of MRI in accretion disks or experiments is left for future work.

ACKNOWLEDGMENTS

Financial support from the Alexander von Humboldt Foundation and the DFG in the framework of STE 991/1-1 and of SFB 609 is gratefully acknowledged.

APPENDIX

A. Bilharz stability criterion

For the polynomial with the complex coefficients

$$\lambda^4 + a_1\lambda^3 + a_2\lambda^2 + (a_3 + ib_3)\lambda + a_4 + ib_4 = 0, \quad \text{(A1)}$$

the Bilharz matrix, B, composed of the coefficients of the polynomial, is [16,19]

$$B = \begin{pmatrix} a_4 & -b_4 & 0 & 0 & 0 & 0 & 0 & 0 \\ b_3 & a_3 & a_4 & -b_4 & 0 & 0 & 0 & 0 \\ -a_2 & 0 & b_3 & a_3 & a_4 & -b_4 & 0 & 0 \\ 0 & -a_1 & -a_2 & 0 & b_3 & a_3 & a_4 & -b_4 \\ 1 & 0 & 0 & -a_1 & -a_2 & 0 & b_3 & a_3 \\ 0 & 0 & 1 & 0 & 0 & -a_1 & -a_2 & 0 \\ 0 & 0 & 0 & 0 & 1 & 0 & 0 & -a_1 \\ 0 & 0 & 0 & 0 & 0 & 0 & 1 & 0 \end{pmatrix}. \quad \text{(A2)}$$

The Bilharz conditions for asymptotic stability require positiveness of the diagonal even-ordered minors of B:

$$\begin{aligned} m_1 &= a_3a_4 + b_3b_4 > 0, \\ m_2 &= (a_2a_3 - a_1a_4)m_1 - a_2^2b_4^2 > 0, \\ m_3 &= (a_1a_2 - a_3)m_2 - \left[a_1^2a_4a_2 + (a_1b_3 - b_4)^2\right]m_1 \\ &\quad + a_1a_4\left[b_4a_2(2b_4 - a_1b_3) + a_1^2a_4^2\right] > 0, \\ m_4 &= a_1m_3 - a_1a_3m_2 + \left(a_3^3 + a_1^2b_4b_3 - 2a_1b_4^2\right)m_1 \\ &\quad + a_1b_4^2a_4(a_1a_2 - a_3) - b_4^2a_3^2a_2 + b_4^4 > 0. \end{aligned} \quad \text{(A3)}$$

In [16] it was shown that when the last of the stability conditions (A3) is fulfilled, the remaining inequalities are satisfied automatically. Therefore, $m_4 = 0$ defines the threshold of HMRI.

B. Routh-Hurwitz stability criterion for SMRI dispersion equation

Putting $\beta = 0$ in the dispersion equation (8), we arrive at the SMRI dispersion equation with the coefficients [16]

$$\begin{aligned} a_1 &= 2(1 + \mathrm{Pm}^{-1})\sqrt{\mathrm{Pm}}, \\ a_2 &= 2(1 + \mathrm{Ha}^2) + 4\mathrm{Re}^2(1 + \mathrm{Ro})\mathrm{Pm} + a_1^2/4, \\ a_3 &= a_1(1 + \mathrm{Ha}^2) + 8\mathrm{Re}^2(1 + \mathrm{Ro})\sqrt{\mathrm{Pm}}, \\ a_4 &= (1 + \mathrm{Ha}^2)^2 + 4\mathrm{Re}^2[1 + \mathrm{Ro}(\mathrm{PmHa}^2 + 1)]. \end{aligned} \quad \text{(A4)}$$

Composing the Hurwitz matrix of the dispersion function of SMRI, which is the real polynomial with the above coefficients, we write the Lienard and Chipart criterion of asymptotic stability [16,19]:

$$a_4 > 0, \; a_2 > 0, \quad a_1 > 0, \quad h_3 = a_1a_2a_3 - a_1^2a_4 - a_3^2 > 0. \quad \text{(A5)}$$

As shown in [16], we get

$$h_3 = 64\left(\mathrm{PmRe}^2(\mathrm{Ro}+1)+\frac{a_1^2}{16}\right)^2 + \mathrm{Ha}^2 a_1^2\left(\frac{a_1^2}{4}+4\mathrm{Re}^2\right) > 0. \quad \text{(A6)}$$

On the other hand, condition $a_4 > 0$ implies that

$$\mathrm{Ro} > -\frac{(1+\mathrm{Ha}^2)^2+4\mathrm{Re}^2}{4\mathrm{Re}^2(\mathrm{PmHa}^2+1)} > -1-\frac{1}{4\mathrm{Re}^2}. \quad \text{(A7)}$$

This means that

$$a_2 > 2(1+\mathrm{Ha}^2)-\mathrm{Pm}+a_1^2/4 = 2(1+\mathrm{Ha}^2)+2+\mathrm{Pm}^{-1}. \quad \text{(A8)}$$

Thus, assuming $\mathrm{Pm} > 0$, which is physically relevant, we automatically have $a_1 > 0$ and $a_2 > 0$. Therefore, four stability conditions (A5) are reduced to the only condition (A7) that yields the threshold of SMRI given by (4).

C. Coefficients of the polynomial Q

The roots of the polynomial

$$Q(\mathrm{Rm},S,\beta,\mathrm{Ro}) = p_0 + p_1\mathrm{Rm}^2 + p_2\mathrm{Rm}^4 + p_3\mathrm{Rm}^6 \quad \text{(A9)}$$

are coefficients of the linear approximation to the domains of the essential HMRI and helically modified SMRI in the $(\mathrm{Rm}^{-1},\mathrm{Pm})$ plane for given β, S, and Ro.

The coefficients of the polynomial Q are

$$p_0 = S^4(4\beta^4S^2+2\beta^2+4S^2\beta^2+1)^2,$$

$$\begin{aligned} p_1 = 4[&-\beta^2(1+20S^4\beta^2+2S^4+8\beta^2S^6+16\beta^6S^6 \\ &+24S^6\beta^4+4S^2+8\beta^2S^2+20\beta^4S^4)\mathrm{Ro}^2 \\ &+(16S^6\beta^4+16\beta^6S^2+S^2+4\beta^4+16\beta^8S^4 \\ &+1-16\beta^8S^6+4S^2\beta^4)\mathrm{Ro} \\ &+1-8S^2\beta^2(S^4\beta^2-\beta^2+S^4-\beta^2S^2+S^2) \\ &+16\beta^6S^2(1+\beta^2S^2+S^2+S^4)+4\beta^4+2S^4], \end{aligned} \quad \text{(A10)}$$

$$\begin{aligned} p_2 = 16[&S^4\beta^4\mathrm{Ro}^4 \\ &-\beta^2(-2+4\beta^4S^4-3S^2+4S^4\beta^2)\mathrm{Ro}^3 \\ &+2\beta^2(3+4\beta^2+6\beta^4S^4+4S^2+16\beta^2S^2+3S^4 \\ &+8S^2\beta^4+12S^4\beta^2)\mathrm{Ro}^2 \\ &+(32\beta^4S^4+16\beta^4+40S^2\beta^4+2+2S^2+4\beta^2 \\ &+32\beta^6S^4+32\beta^6S^2)\mathrm{Ro} \\ &+2+4S^4\beta^2+8S^2\beta^4+16\beta^6S^2 \\ &+8\beta^4+16\beta^6S^4+S^4+4\beta^4S^4], \end{aligned}$$

$$\begin{aligned} p_3 = 64[&(2\mathrm{Ro}\beta^2+1)^2+8\mathrm{Ro}\beta^4+4\beta^4+3\mathrm{Ro}^2\beta^2 \\ &-\mathrm{Ro}^3\beta^2](\mathrm{Ro}+\mathrm{Ro}S^2+1). \end{aligned}$$

D. Explicit form of the discriminant

The discriminant equation for the polynomial Q is $64p_0p_3\Delta^2$, where

$$\Delta(S,\beta,\mathrm{Ro}) := 18p_0p_1p_2p_3 - 4p_1^3p_3 + p_1^2p_2^2 - 4p_0p_2^3 - 27p_0^2p_3^2. \quad \text{(A11)}$$

The function Δ further factors as

$$\Delta = 4096\beta^2\Delta_1^2\Delta_2, \quad \text{(A12)}$$

where

$$\begin{aligned} \Delta_1 = &-\beta^2S^2(2\beta^2S^2+1)(2\beta^2S^2+2S^2+1)\mathrm{Ro}^3 \\ &+[16\beta^6S^4(2+\beta^2S^2)+(1+S^2)^2 \\ &+20S^2\beta^2(\beta^2+2\beta^4S^4+S^2) \\ &+2\beta^2(2+9S^2)+4\beta^4S^4(13+7S^2)]\mathrm{Ro}^2 \\ &+4\beta^2(1+12\beta^6S^6+4S^2+5S^6+18S^4\beta^2 \\ &+16\beta^4S^4+7\beta^2S^2+5S^4 \\ &+11S^6\beta^2+20\beta^4S^6)\mathrm{Ro} \\ &+4S^2(8\beta^6S^2+2\beta^4+2S^4\beta^2 \\ &+8\beta^6S^4+1+4\beta^4S^2 \\ &+6\beta^4S^4+S^4+4\beta^2S^2+8\beta^8S^4+2S^2), \end{aligned} \quad \text{(A13)}$$

$$\begin{aligned} \Delta_2 = &16S^8\beta^4(1+\mathrm{Ro})^2 \\ &\times[(\mathrm{Ro}+4)(\beta^2+1)\beta^4\mathrm{Ro}^3-11\mathrm{Ro}\beta^2(\mathrm{Ro}+2) \\ &+4\beta^6\mathrm{Ro}^2-8\mathrm{Ro}^2\beta^4-24\mathrm{Ro}\beta^4-(1+4\beta^2)^2] \\ &+S^6(-4-128\mathrm{Ro}\beta^{10}-240\mathrm{Ro}^4\beta^6-1312\mathrm{Ro}^3\beta^8 \\ &-256\beta^{10}\mathrm{Ro}^2+152\mathrm{Ro}^5\beta^6+280\mathrm{Ro}^5\beta^8+8\mathrm{Ro}^6\beta^8 \\ &+96\beta^{10}\mathrm{Ro}^5+240\mathrm{Ro}^4\beta^8-1960\mathrm{Ro}^3\beta^6-156\beta^4\mathrm{Ro}^4 \\ &+4\mathrm{Ro}^6\beta^6+16\beta^4-2240\beta^8\mathrm{Ro}-2912\beta^6\mathrm{Ro}^2 \\ &+144\mathrm{Ro}\beta^4-1568\mathrm{Ro}\beta^6-224\beta^6-640\beta^8 \\ &-296\beta^4\mathrm{Ro}^3-2880\beta^8\mathrm{Ro}^2-96\mathrm{Ro}\beta^2+192\beta^{10}\mathrm{Ro}^4 \\ &-32\beta^{10}\mathrm{Ro}^3-60\mathrm{Ro}^2\beta^2-24\beta^2-24\mathrm{Ro}^2\beta^4) \\ &+S^4(12-64\mathrm{Ro}\beta^{10}+44\mathrm{Ro}^4\beta^6-832\mathrm{Ro}^3\beta^8 \\ &-560\beta^{10}\mathrm{Ro}^2-78\mathrm{Ro}^3\beta^2+164\mathrm{Ro}^5\beta^6+120\mathrm{Ro}^5\beta^8 \\ &-104\mathrm{Ro}^4\beta^8-944\mathrm{Ro}^3\beta^6-118\beta^4\mathrm{Ro}^4+\mathrm{Ro}^6\beta^6 \\ &+64\beta^{10}-640\beta^8\mathrm{Ro}-2008\beta^6\mathrm{Ro}^2+30\mathrm{Ro}^5\beta^4 \\ &-240\mathrm{Ro}\beta^4-1664\mathrm{Ro}\beta^6-480\beta^6-192\beta^8 \\ &-472\beta^4\mathrm{Ro}^3-1056\beta^8\mathrm{Ro}^2+12\mathrm{Ro}-156\mathrm{Ro}\beta^2 \\ &-27\mathrm{Ro}^4\beta^2-240\beta^{10}\mathrm{Ro}^4-672\beta^{10}\mathrm{Ro}^3 \\ &-155\mathrm{Ro}^2\beta^2-60\beta^2-584\mathrm{Ro}^2\beta^4) \\ &+4S^2(4\mathrm{Ro}\beta^4+4\beta^4-\mathrm{Ro}^2\beta^2+1+\mathrm{Ro}) \\ &\times(8\beta^6\mathrm{Ro}^2+16\mathrm{Ro}\beta^6+8\beta^6-10\beta^4\mathrm{Ro}^3-10\mathrm{Ro}^2\beta^4 \\ &+4\mathrm{Ro}\beta^4+4\beta^4-6\mathrm{Ro}^3\beta^2-11\mathrm{Ro}^2\beta^2-12\mathrm{Ro}\beta^2 \\ &-6\beta^2-3\mathrm{Ro}-3) \\ &+4(1+\mathrm{Ro})(4\mathrm{Ro}\beta^4+4\beta^4-\mathrm{Ro}^2\beta^2+1+\mathrm{Ro})^2. \end{aligned} \quad \text{(A14)}$$

[1] E. P. Velikhov, Sov. Phys. JETP USSR **9**, 995 (1959).
[2] S. Chandrasekhar, PNAS **46**, 253 (1960).
[3] S. A. Balbus and J. F. Hawley, Astrophys. J. **376**, 214 (1991).
[4] I. Herron, Anal. Appl. **2**, 145 (2004).
[5] E. Knobloch, Astrophys. J. **376**, 214 (1991); R. Hollerbach and G. Rüdiger, Phys. Rev. Lett. **95**, 124501 (2005).
[6] S. A. Balbus and J. F. Hawley, Rev. Mod. Phys. **70**, 1 (1998).
[7] D. R. Sisan, N. Mujica, W. A. Tillotson, Y. M. Huang, W. Dorland, A. B. Hassam, T. M. Antonsen, and D. P. Lathrop, Phys. Rev. Lett. **93**, 114502 (2004); F. Stefani, T. Gundrum, G. Gerbeth, G. Rudiger, M. Schultz, J. Szklarski, and R. Hollerbach, *ibid.* **97**, 184502 (2006); F. Stefani, G. Gerbeth, T. Gundrum, R. Hollerbach, J. Priede, G. Rudiger, and J. Szklarski, Phys. Rev. E **80**, 066303 (2009); M. D. Nornberg, H. Ji, E. Schartman, A. Roach, and J. Goodman, Phys. Rev. Lett. **104**, 074501 (2010).
[8] J. W. S. Rayleigh, Proc. R. Soc. London A **93**, 148 (1917).
[9] S. A. Balbus, Ann. Rev. Astron. Astroph. **41**, 555 (2003).
[10] D. J. Acheson and R. Hide, Rep. Prog. Phys. **36**, 159 (1973); A. P. Willis and C. F. Barenghi, Astron. Astrophys. **388**, 688 (2002); D. A. Shalybkov, Phys. Usp. **52**, 915 (2009); H. Goedbloed, R. Keppens, and S. Poedts, *Advanced Magnetohydrodynamics* (Cambridge University Press, Cambridge, UK, 2010).
[11] J. Priede, I. Grants, and G. Gerbeth, Phys. Rev. E **75**, 047303 (2007); J. Phys.: Conf. Ser. **64**, 012011 (2007).
[12] W. Liu, J. Goodman, I. Herron, and H. Ji, Phys. Rev. E **74**, 056302 (2006).
[13] G. Rüdiger and R. Hollerbach, Phys. Rev. E **76**, 068301 (2007).
[14] O. M. Umurhan, Astron. Astrophys. **513**, A47 (2010).
[15] H. Ji, J. Goodman and A. Kageyama, MNRAS **325**, L1 (2001); V. Urpin and G. Rüdiger, Astron. Astrophys. **437**, 23 (2005); V. P. Lakhin and E. P. Velikhov, Phys. Lett. A **369**, 98 (2007); G. Rüdiger and M. Schultz, Astron. Nachr. **329**, 659 (2008).
[16] O. N. Kirillov and F. Stefani, Astrophys. J. **712**, 52 (2010).
[17] V. I. Arnold, Russ. Math. Surv. **26**, 29 (1971); S. A. van Gils, M. Krupa, and W. F. Langford, Nonlinearity **3**, 825 (1990); O. N. Kirillov, Dokl. Phys. **49**, 239 (2004); O. N. Kirillov, Dokl. Math.**76**, 780 (2007); R. Krechetnikov and J. E. Marsden, Rev. Mod. Phys. **79**, 519 (2007); O. N. Kirillov and F. Verhulst, Z. Angew. Math. Mech. **90**, 462 (2010).
[18] G. W. Hill, Am. J. Math. **1**, 5 (1878); V. V. Sidorenko and A. Celletti, Cel. Mech. Dyn. Astron. **107**, 209 (2010).
[19] H. Bilharz, Z. Angew. Math. Mech. **24**, 77 (1944).
[20] I. Hoveijn and O. N. Kirillov, J. Diff. Eqns. **248**, 2585 (2010).